

SHAOBAI LI  
JUNGENG FAN  
SHUANG XU  
RUNDONG LI  
JINGDE LUAN

College of Energy and  
Environment and Liaoning Key  
Laboratory of Clean Energy,  
Shenyang Aerospace University,  
Shenyang, China

SCIENTIFIC PAPER

UDC 66.021.3:532.516:544

## THE INFLUENCE OF pH ON GAS-LIQUID MASS TRANSFER IN NON-NEWTONIAN FLUIDS

### Article Highlights

- The mass transfer process of bubble swarms in non-Newtonian fluids was studied experimentally
- The  $k_L a$  increased with the gas flow rate and decreased with the apparent viscosity of the liquid
- The pH value exhibited a marginal effect on the gas-liquid mass transfer for  $\text{pH} < 7$
- The gas-liquid mass transfer rate increased with increasing pH for  $\text{pH} > 7$

### Abstract

*In this study, the effect of pH on the mass transfer of oxygen bubble swarms in non-Newtonian fluids was experimentally studied. The volumetric liquid side mass transfer coefficient ( $k_L a$ ), liquid side mass transfer coefficient ( $k_L$ ), and specific interfacial area ( $a$ ) were investigated. The pH was regulated by the addition of hydrochloric acid and sodium hydroxide (NaOH). It was found that the  $k_L a$  increased with the gas flow rate increasing and decreased with the apparent viscosity of the liquid increasing. In the case of  $\text{pH} < 7$ , a marginal effect of pH on the gas-liquid mass transfer was observed, but when pH value was higher than 7, mass transfer was promoted with the increase of pH value. Via investigating the impact of pH on  $k_L$  and  $a$ , the variation of mass transfer at  $\text{pH} > 7$  was attributed to the decomposition of the Xanthan molecular structure by the hydroxyl of NaOH.*

*Keywords: bubble swarms, xanthan gum solution, non-Newtonian fluids, pH, mass transfer.*

Mass transfer between dispersed bubble swarms and continuous liquid phase is widely encountered in various biotechnological processes, such as food fermentation, sludge anaerobic digestion, and biological wastewater treatment [1]. Mass-transfer efficiency is decisive to those biological processes mentioned above [2]. Hence, in recent years, considerable research efforts have been devoted to the mass transfer of bubble swarms in Newtonian fluids. These studies mainly focus on the effect of different parameters on mass transfer, including gas flow rate

[3], temperature [4], bubble column diameter [5], density and loading [6], liquid properties [7-8], and geometrical characteristics of sparger design [9].

However, notably, the vast majority of the materials encountered in biological processes exhibit non-Newtonian characteristics [10]. Owing to complex rheological properties, the mass transfer of bubble swarms in those fluids is more intricate, which attracts the interest of many researchers. Gómez-Díaz *et al.* [11,12] have investigated gas-liquid mass transfer in shear-thinning fluids and analyzed the effect of the gas flow rate and solution concentration on mass transfer. They also proposed a correlation for predicting the interface area and gas hold up of bubble swarms rising in non-Newtonian fluids. Garcia-Ochoa [13] has investigated the mass transfer phenomenon of rising oxygen bubbles in xanthan gum solutions and proposed a mass-transfer correlation by introducing shear viscosity. Li *et al.* [14] have investigated the mass transfer of

Correspondence: S. Li, College of Energy and Environment and Liaoning Key Laboratory of Clean Energy, Shenyang Aerospace University, Shenyang, 110136, China.

E-mail: lishaobai1982@163.com

Paper received: 5 July, 2016

Paper revised: 12 September, 2016

Paper accepted: 26 September, 2016

<https://doi.org/10.2298/CICEQ160705046L>

carbon dioxide bubble swarms in three rheological fluids (Newtonian fluids, shear thinning fluids and viscoelastic fluids) and further developed a semi-theoretical model based on Higbie's penetration theory and Kolmogorov's theory of isotropic turbulence.

Despite all these studies, the available information about the gas liquid mass transfer in non-Newtonian fluids is still insufficient, especially, in more complex biological processes in which the liquid phase exhibits non-Newtonian behavior. pH is well known to be one of the most important parameters, which should be optimized to promote the product yield. Thus, HCl or NaOH aqueous solutions are usually added to the bioreactors and fermentors for neutralizing the generated bases or acids, by which the pH is maintained to an optimum biological value [15]. Although, the effect of pH on the gas liquid mass transfer is imperative in biological processes, marginal experimental data is observed in past studies.

Xanthan is a typical non-Newtonian fluid, and its apparent viscosity exhibits shear thinning behavior. Xanthan is utilized in many practical fields, for example being added into foods as thickener and employed as polymer-flooding agent for enhancing oil recovery [16]. In this study, the effect of pH on the gas-liquid mass transfer in a xanthan solution was experimentally investigated. The volumetric mass transfer coefficient and interfacial area were respectively determined using an oxygen probe and by the photographic method. The effects of pH, liquid concentration, and gas flow rate on the volumetric mass-transfer coefficient, interfacial area, and mass-transfer coefficient were systematically analyzed.

## EXPERIMENTAL

### Experimental apparatus and procedure

The experimental set-up (Figure 1) consisted of cylindrical Plexiglas tanks (with an internal diameter of 0.08 m and a height of 1 m) surrounded by a square duct (0.1 m×0.1 m×1 m). The square duct serves to eliminate optical distortions for visualization. Two orifices with a diameter of 2 mm were submerged in the liquid in the bottom section of the tanks: an oxygen inlet and a nitrogen inlet. Before the beginning of the experiment, the cylindrical plexiglas bubble column and its external rectangular plexiglas sink were first filled with Xanthan solution to 750 mm under the specific condition. Next, nitrogen was added into the bubble column for desorption of oxygen from the liquid phase. Meanwhile, the concentration of oxygen in liquids was measured using a calibrated oxygen sensor (FC-100: ASR Co., Ltd.), which was located at 500 mm above

the nozzle. Because of the disturbance of bubbles, the distribution of oxygen concentration becomes homogeneous within a few seconds, *i.e.*, the readings from the oxygen sensor can be considered as the actual oxygen concentration in the bulk liquids. The ventilated process of nitrogen was stopped when the readings of the oxygen sensor goes to zero. After standing for 30 min, the nitrogen inlet valve was switched off, and the oxygen inlet valve was opened and controlled by a calibrated rotameter. The dissolved oxygen concentration was recorded at 1 min intervals. The bubbles were determined using a high-speed camera with a resolution of 500×1728 pixels. On these obtained images, at least 60 well-defined bubbles were used to calculate the Sauter mean diameter of bubbles and specific interfacial area at different conditions. A self-written program was operated on Matlab 6.0 to obtain the necessary geometric characteristics of the bubbles. In this experiment, the selected gas flow rate was 10, 15, 20 and 25 L/h, and the selected pH values were 3, 4, 5, 6, 7, 8, 9, 10 and 11. All experiments were conducted at room temperature under constant pressure.

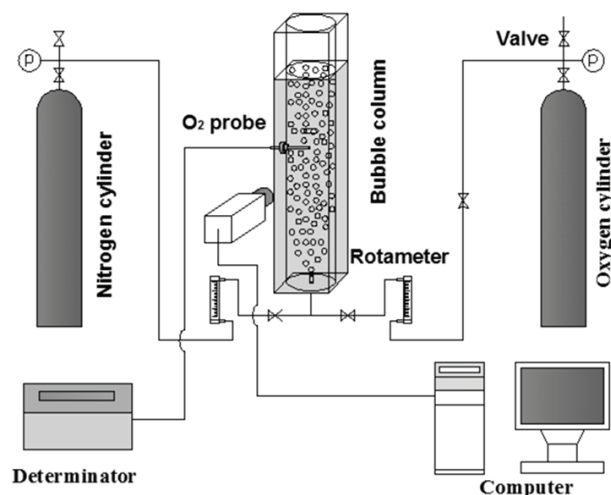


Figure 1. Schematic representation of experimental apparatus.

### Materials

In this study, different concentrations of xanthan solutions (0.2, 0.4, 0.6, 0.8 and 1.0 wt.%) were used as experimental liquids. Analytical-purity xanthan (analytical purity, type KX-F supplied by Tianjin Kermel Chemical Reagent Co. (Tianjin, China)) and double-distilled deionized water were used in the experiments. The experimental liquid density was measured using a balance hydrometer. Rheology properties were measured using a Brookfield viscometer (Brookfield, DV-III, USA) with a shear rate ranging from 0.1 to 1000 s<sup>-1</sup>. As can be seen in Figure 2, all of the xanthan solutions exhibit shear thinning behavior. The variation of the

apparent viscosity of xanthan solutions is well represented by the power-law model [17]:

$$\mu = K\gamma^{n-1} \quad (1)$$

where  $K$  is the consistency index, and  $n$  is the flow index.

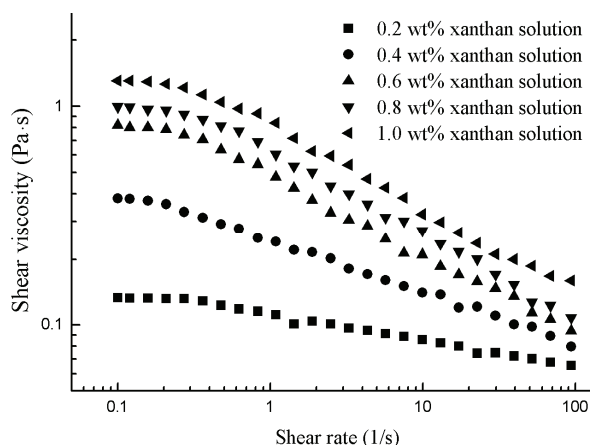


Figure 2. Variation of the viscosity of the different fluids used in the present study.

Table 1 summarizes the liquid physical properties.

Table 1. Rheological and physical properties of experimental fluids

Fluid, xanthan content, wt. %	$K / \text{Pa}\cdot\text{s}^n$	$n$	$\rho / \text{kg m}^{-3}$
0.2	0.13	0.88	996.32
0.4	0.25	0.77	997.65
0.6	0.51	0.67	1006.44
0.8	0.64	0.63	1008.24
1.0	0.85	0.59	1010.43

## RESULTS AND DISCUSSION

In the mass-transfer process, the experimental data of oxygen concentration obtained in the bulk of the liquid phase increases with time increasing until the liquid phase is saturated. Based on mass balance, the liquid phase volumetric mass transfer coefficient ( $k_L a$ ) can be defined as follows:

$$\frac{dC}{dt} = k_L a (C^* - C) \quad (2)$$

here,  $k_L a$  represents the volumetric liquid-side mass transfer coefficient, and  $C^*$  and  $C$  represent the solubility and instantaneous oxygen concentration, respectively. Integrating Eq. (2), Eq. (3) is obtained:

$$\ln\left(\frac{C^*}{C^* - C}\right) = k_L a t \quad (3)$$

Using the experimental data of instantaneous oxygen concentration at different times,  $k_L a$  is calculated by linear regressions. Figure 3 shows the effect of the gas flow rate and xanthan concentration upon the mass transfer of oxygen to the liquid phase at pH 7, representing the effect based on  $k_L a$ . As can be observed from Figure 3,  $k_L a$  increases with the increase of flow rate and the decrease the xanthan concentration. Similar results have been obtained using different non-Newtonian fluids in the liquid phase in previous studies [14,18,19]. The effect of the gas flow rate could be attributed to the enhancement of the liquid turbulence and enlargement of the interfacial area. Figure 2 shows the rheological curve of Xanthan solutions, where the apparent viscosity of Xanthan solutions increases with increasing concentration. The study of Alvarez *et al.* [20] has revealed that viscosity increases the resistance of mass transfer and decreases the turbulence of liquids. Thus,  $k_L a$  decreases with increasing concentration of the xanthan solution, as shown in Figure 3. Accordingly,  $k_L a$  is not sensitive to the gas flow rate in highly viscous liquids, which may be attributed to the coalescence of bubbles in highly viscous liquid at high gas flow rate. The coalescence of bubbles increases the size of the bubbles, which results in the decrease of the residence time, the gas holdup and  $k_L a$ , and ultimately offsets the increase of mass transfer by increasing the gas flow rate [12].

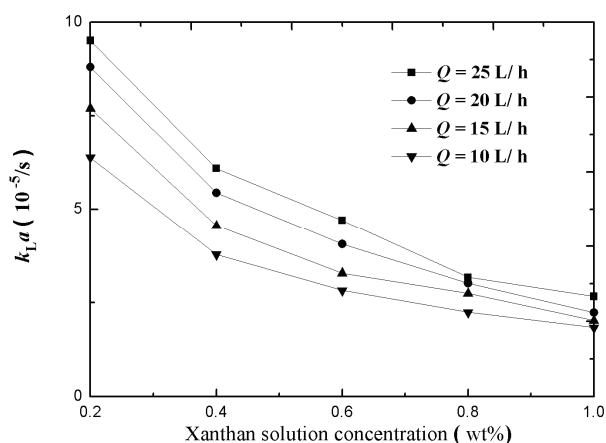


Figure 3. Influence of xanthan solution concentration and gas flow rate on  $k_L a$ .

Figure 4 shows the variation of  $k_L a$  with pH at  $Q = 20$  L/h. At pH < 7, it can be seen from Figure 4 that no apparent change of  $k_L a$  can be found with the regulation of pH. Thus, it seems that HCl exerts almost no effect on the gas-liquid mass transfer in xanthan solutions. On the other hand,  $k_L a$  clearly increases with increasing pH value at pH > 7 as shown in Figure 4, and the increasing trend is further enhanced as the

concentration increases, indicating that addition of NaOH solution can promote the gas-liquid mass transfer in Xanthan solutions and this effect increases with solution concentration.

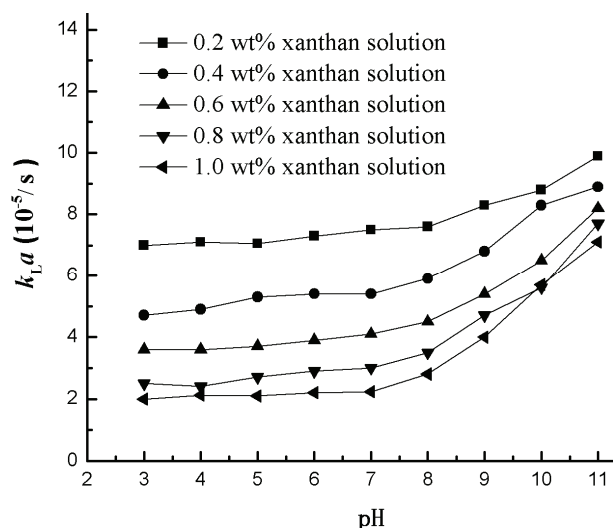


Figure 4. Influence of pH on  $k_L a$  at  $Q = 20$  L/h for different concentration xanthan solution.

Although  $k_L a$  is more general for dealing with the mass transfer of bubble swarms in a two-phase flow, it only reflects the effect of operation conditions upon the gas-liquid mass transfer and cannot explain the related influence mechanism.  $k_L a$  is the combination of the mass transfer coefficient ( $k_L$ ) and interfacial area ( $a$ ). Thus, it is necessary to separately consider the values of  $k_L$  and  $a$  to obtain more information about the effect of pH on global mass transfer. However, it is very difficult to acquire the value of  $a$  in industry. In this study, the bubble column is fabricated with Plexiglas, and the liquid phase is transparent. Hence, information of the bubble size could be obtained from the methodology developed by Ferreira *et al.* [21].

The bubbles rising in the Xanthan solution are ellipsoidal. Hence, major ( $d_h$ ) and minor ( $d_v$ ) axes of the projected ellipsoid (in two dimensions) were determined. The diameter of the equivalent sphere was taken as the representative bubble dimension:

$$d = \sqrt[3]{d_h^2 d_v} \quad (4)$$

As the bubble swarms freely rise through liquids, the distribution of the bubble size is well represented by the Sauter mean diameter ( $d_{32}$ ), expressed as follows:

$$d_{32} = \frac{\sum_i (n_i d_i^3)}{\sum_i (n_i d_i^2)} \quad (5)$$

here,  $n_i$  is the number of bubbles, which have the same equivalent diameter ( $d_i$ ).

The gas hold up values was obtained by visual observation [22]. In this case, the total gas holdup,  $\phi$  is defined as follows:

$$\phi = \frac{H - H_L}{H} \quad (6)$$

where  $H_L$  is the clear liquid height, and  $H$  is the liquid dispersion height attributed to the presence of bubble swarms. The results represent the average values of five repeated experiments under same conditions, and experimental data were reproducible to within  $\pm 5\%$ .

The specific interfacial area,  $a$ , can be obtained from  $\phi$  and  $d_{32}$  as follows [23]:

$$a = \frac{6\phi}{d_{32}(1-\phi)} \quad (7)$$

Figure 5 shows the bubbles size distribution under different gas flow rate at pH 7, based on the diameter of the equivalent sphere. It can be observed from Figure 5 that the bubble size has a normal distribution, and the degree of bubble size dispersion increases with the gas flow rate elevated due to the increase of bubble-coalescing frequency at high gas flow rate.

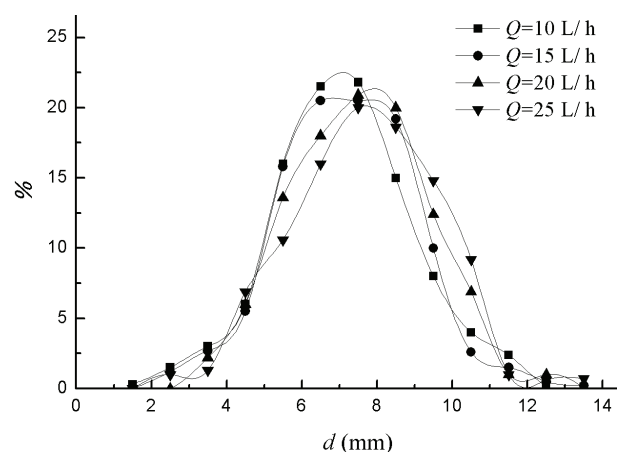


Figure 5. The bubbles size distribution under different gas flow rate for pH 7.

Figure 6 shows the effect of pH and the xanthan solution concentration on the specific interfacial area ( $a$ ) at  $Q = 20$  L/h. As shown in Figure 6 the specific interfacial increases with the decreased concentration of xanthan solution. Similar results were reported in the studies conducted by Gómez-Díaz *et al.* [12] and Li *et al.* [14]. Gómez-Díaz *et al.* [12] have attributed the decrease to the difficulty for the bubble to ascend in the high-viscosity liquid phase and produce the increment

of bubble size, followed by a clear decrease of the specific interfacial area. Li *et al.* [14] have proposed that the rheological property of liquid phase significantly affects the specific interfacial area. According to Li *et al.* [24], when bubbles rise in shear-thinning fluids, even two bubbles with a specifically long distance, the shear-thinning effect caused by the passage of the leading bubble can provide a reduced local viscosity, resulting in the decrease in the drag force opposing the trailing bubble. Namely, two bubbles coalescing in non-Newtonian fluids is an accelerating process as compared to that in Newtonian fluids. Typically, large bubbles have a short residence time and small specific surface area, which consequently causes decrease on the specific interfacial area with the increased concentration of xanthan solution. From Figure 6,  $a$  increases with increasing pH at pH > 7 but remains constant at pH < 7. The variation is assumed to be related to the change on the xanthan molecular structure. In fact, bases react with the acetyl group of xanthan molecules and decrease the viscosity of xanthan solution [25]. The rheological property of 0.6 wt.% xanthan solution at different pH was measured in order to evidence the hypothesis above, and the results are shown in Table 2. Notably,  $K$  decreases and  $n$  increases with increasing pH at pH > 7 but both  $K$  and  $n$  remain approximately constant at pH ≤ 7. According to the study by Weissenborn *et al.* [26], there is no difference expected between acid and alkali on  $a$ , as no significant differences on liquid properties are observed. Their results are consistent with those in our study at pH < 7, in which the xanthan molecular structure is not destroyed by HCl. This is consistent with the variation of bubble size distributions with three different pH values in 0.6 wt.% xanthan solution and at  $Q = 20$  L/h (Figure 7). The experimental data plotted in Figure 7 indicate that there is not a clear influence of the pH values upon the bubbles size distribution for pH 3 and 7, but smaller bubbles are observed for pH 10.

$k_L a$  is composed of the mass transfer coefficient ( $k_L$ ) and the interfacial area ( $a$ ). Once the information of the specific interfacial area ( $a$ ) could be calculated, the mass-transfer coefficient ( $k_L$ ) can be obtained from the production of  $k_L a$  divided by  $a$ . Figure 8 shows the effect of pH on the mass-transfer coefficient ( $k_L$ ) for xanthan solutions of different concentrations. From Figure 8, the variation of  $k_L$  is basically the same as that of  $k_L a$ . At pH < 7, no significant change of  $k_L$  can be noticed in the range of experiments. Nevertheless,  $k_L$  increases with the increased pH at pH > 7, and the higher concentration of xanthan solutions, the larger of the increase trend, which could be attributed to the variation of the xan-

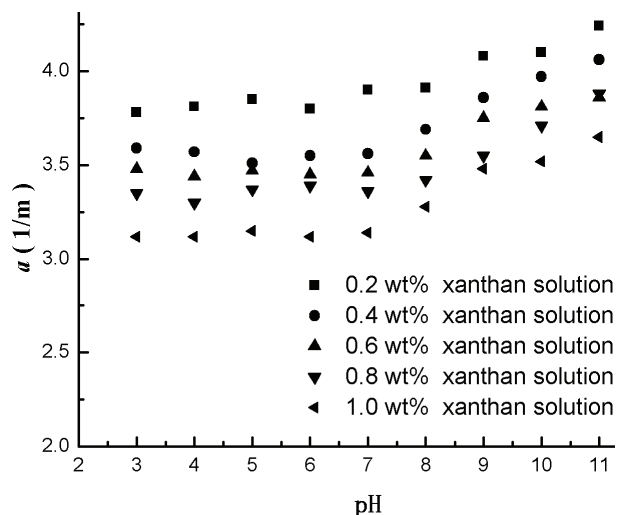


Figure 6. Influence of pH upon gas-liquid specific interfacial area ( $Q = 20$  L/h).

Table 2. Rheological property of 0.6 wt.% xanthan solution at different pH

pH	$K$ / Pa·s <sup><i>n</i></sup>	$n$
3	0.51	0.65
5	0.52	0.69
7	0.51	0.68
9	0.38	0.74
11	0.24	0.88

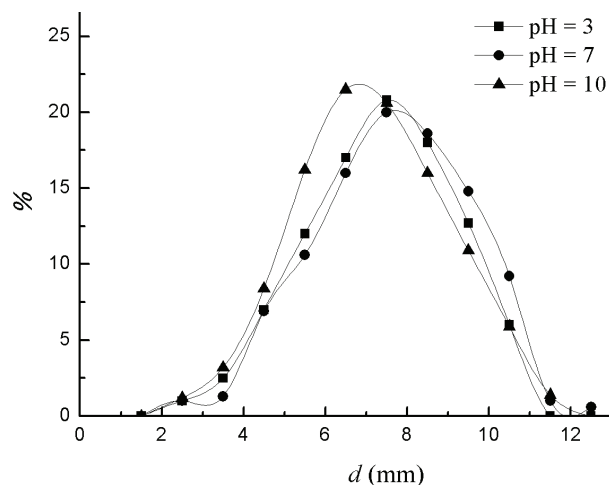


Figure 7. The bubble size distributions with three different pH values in 0.6 wt.% xanthan solution and at  $Q = 20$  L/h.

than solution caused by the addition of acids and bases. According to the result in Table 2, HCl marginally affects the rheological property of Xanthan solutions, which indicates that HCl will not destroy the molecular structure of xanthan. However, the rheological property of the xanthan solutions decreases because of the destruction of the Xanthan molecular structure by NaOH, resulting in the decrease of appa-

rent viscosity. Xanthan monomer is a molecule consisting of D-glucose, D-mannose, D-glucuronic acid, pyruvic acid and acetyl. Therefore, acetyl has a significant effect on the spatial conformation of xanthan molecule, thus affecting the xanthan solution rheology [27]. Abundant studies have demonstrated that sodium hydroxide could remove the acetyl group of xanthan molecules. The reaction mechanism is as follows [28]:

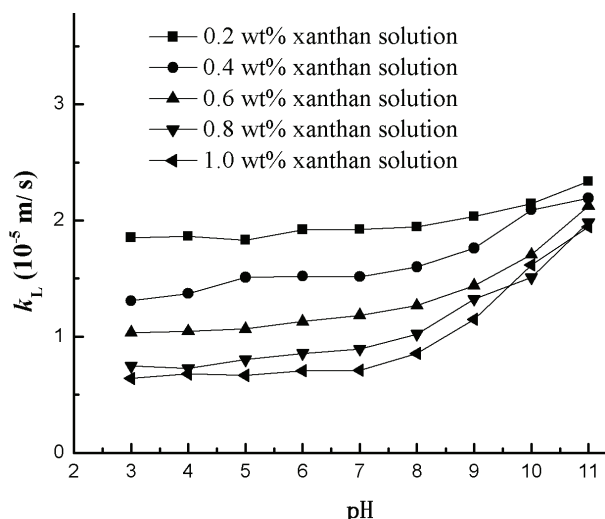
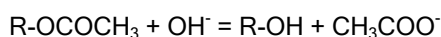


Figure 8. Influence of pH on the gas-liquid mass transfer coefficient.

As the amount of sodium hydroxide increasing, the acetyl group content on xanthan molecules decreased, which lead to the decrease of rheological property and apparent viscosity. As reported by Alvarez *et al.* [20], the decrease of apparent viscosity is able to cause the increase of  $k_L$ . Ferreira *et al.* [29] have investigated the effect of pH on the oxygen mass-transfer coefficient in distilled water and found that  $k_L$  exhibits higher values in solutions with  $\text{pH} < 7$  and  $\text{pH} > 7$  as compared with those in distilled water, which is different from the result obtained herein. According to the study of Ferreira, the variation of  $k_L$  in different pH systems is attributed to the bubble surface contamination. However, in our study, the high-viscosity Xanthan solution was used as the liquid phase. Similar to the work of Tzounakos [30], a competition between the molecules of carboxymethyl cellulose (CMC) and surfactant molecules exists on the bubble surface: CMC allows less surfactant molecules to reach the bubble surface. Thus, no discernible effect by the acid is revealed on  $k_L$  and  $a$  without breaking xanthan molecular structure, the phenomenon can be attributed to the preventing electrolyte molecule from accumulating on the bubble

surface by xanthan molecules. Thus, the variation of  $k_L$  in the system used by Ferreira *et al.* does not exist in the xanthan solution.

## CONCLUSIONS

The mass transfer from oxygen bubble swarms in the xanthan solutions was investigated at different pH values, in order to analyze the effect of pH on the gas-liquid mass transfer in non-Newtonian fluids. The results obtained show that HCl has a marginal effect on mass transfer, but NaOH has a significant influence, which can be related to the increase of  $k_L$  and  $a$ . The variation of the liquid-phase mass transfer coefficient ( $k_L$ ) and  $a$  are possibly related to the viscosity of the liquid phase. At  $\text{pH} < 7$ , no significant change on the rheological property was observed, indicating that HCl does not destroy the structure of the Xanthan molecule. Nevertheless, at  $\text{pH} > 7$ , the rheological property of the xanthan solutions changed because of the destruction of the xanthan molecular structure by base, resulting in the decrease of apparent viscosity. The study of the effect of pH on the gas-liquid mass transfer could provide essential information to the optimization of biological processes.

## Acknowledgements

The Project supported by the National Natural Science Foundation of China (Grant No. 21406141), the Scientific Research Starting Foundation for Doctors of Liaoning Province, China (Grant No. 20141078), the Research Foundation of Education Bureau of Liaoning Province, China (Grant No. L2014060)

## Nomenclature

$a$	specific interfacial area ( $\text{m}^2/\text{m}^3$ )
$C$	concentration of oxygen in liquid (mol/L)
$C^*$	saturation concentration of oxygen in liquid (mol/L)
$a_{32}$	Sauter mean diameter (m)
$H$	height of gas-free liquid (m)
$H_L$	height of the gas-liquid dispersion (m)
$K$	consistency index in a power-law model ( $\text{Pa}\cdot\text{s}^n$ )
$k_L$	liquid-side mass transfer coefficient (m/s)
$n$	flow index in a power-law model
$Q$	volumetric gas flow rate (L/h)
$t$	Time (s)
$\phi$	gas hold up
$\gamma$	shear rate (1/s)
$\mu$	viscosity of liquid phase ( $\text{Pa}\cdot\text{s}$ )
$\rho$	liquid phase density ( $\text{kg}/\text{m}^3$ )

## REFERENCES

- [1] R.P. Chhabra, Bubbles, drops, and particles in non-Newtonian fluids, CRC, Taylor & Francis, New York, 2007, p. 2
- [2] J.Y. Jing, J. Feng, W.Y. Li, Asia-Pac. J. Chem. Eng. **4** (2009) 618-623
- [3] L.K. Ishkintana, C.P.J. Bennington, Can. J. Chem. Eng. **88** (2010) 322-328
- [4] A. Ferreira, C. Ferreira, J.A. Teixeira, F. Rocha, Chem. Eng. J. **162** (2010) 743-752
- [5] X. Su, P.D. Hol, S.M. Talcott, A.K. Staudt, T.J. Heindel, Chem. Eng. Sci. **61** (2006) 3098-3104
- [6] P. Mena, A. Ferreira, J. A. Teixeira, F. Rocha, Chem. Eng. Process. **50** (2011) 181-188
- [7] X. Li, C. Zhu, Chem. Ind. Chem. Eng. Q. **22** (2015) 85-93
- [8] V. Sivasubramanian, Asia-Pac. J. Chem. Eng. **5** (2010) 361-368
- [9] N.A. Kazakis, A.A. Mouza, S.V. Paras, Chem. Eng. J. **137** (2008) 265-281
- [10] R.P. Chhabra, J.F. Richardson, Fluid Dyn. Res. **5** (1999) 147-158
- [11] D. Gómez-Díaz, J. M. Navaza, Chem. Eng. Technol. **26** (2003) 1068-1073
- [12] D. Gómez-Díaz, J.M. Navaza, L.C. Quintáns-Riveiro, Chem. Eng. J. **146** (2009) 16-21
- [13] F. Garcia-Ochoa, E. Gomez, Chem. Eng. Sci. **59** (2004) 2489-2501
- [14] S. Li, C. Zhu, T. Fu, Y. Ma, Int. J. Heat Mass Transfer. **55** (2012) 6010-6016
- [15] S.Y. Lee, Y.P. Tsui, Chem. Eng. Prog. **95** (1999) 23-49
- [16] B. Katzbauer, Polym. Degrad. Stab. **59** (1998) 81-84
- [17] W.R. Schowalter, AIChE J. **6** (1960) 24-28
- [18] A. Tecante, L. Choplin, Can. J. Chem. Eng. **71** (1993) 859-865
- [19] G. Diego, J.M. Navaza, J. Chem. Technol. Biotechnol. **79** (2004) 1105-1112
- [20] E. Álvarez, B. Sanjurjo, A. Cancela, J.M. Navaza, Chem. Eng. Res. Des. **78** (2000) 889-893
- [21] A. Ferreira, G. Pereira, J.A. Teixeira, F. Rocha, Chem. Eng. J. **180** (2012) 216-228
- [22] A.D. Anastasiou, A.D. Passos, A.A. Mouza, Chem. Eng. Sci. **98** (2013) 331-338
- [23] P.H. Calderbank, M.B. Moo-Young, Chem. Eng. Sci. **16** (1961) 39-54
- [24] H.Z. Li, Chem. Eng. Sci. **54** (1999) 2247-2254
- [25] F. García-Ochoa, V.E. Santos, J.A. Casas, E. Gómez, Biotechnol. Adv. **18** (2000) 549-57
- [26] P.K. Weissenborn, R.J. Pugh, J. Colloid Interface Sci. **184** (1996) 550-563
- [27] F. García-Ochoa, V.E. Santos, J.A. Casas, E. Gómez, Biotechnol. Adv. **18** (2000) 549-579
- [28] F. Callet, M. Milas, M. Rinaudo, Int. J. Biol. Macromol. **9** (1987) 291-293
- [29] A. Ferreira, P. Cardoso, J.A. Teixeira, F. Rocha, Chem. Eng. Sci. **100** (2013) 145-152
- [30] A. Tzounakos, D.G. Karamanev, A. Argyrios Margaritis, M.A. Bergougnou, Ind. Eng. Chem. Res. **43** (2004) 5790-5795.

SHAOBAI LI  
JUNGENG FAN  
SHUANG XU  
RUNDONG LI  
JINGDE LUAN

College of Energy and Environment  
and Liaoning Key Laboratory of Clean  
Energy, Shenyang Aerospace  
University, Shenyang, China

NAUČNI RAD

## UTICAJ pH NA PRENOS MASE GAS-TEČNOST U NENJUTNOVSKIM FLUIDIMA

*U ovom radu je eksperimentalno istraživana uticaj pH na prenos mase kiseonika u disperziji gasnih mehurova u nenjutnovskim fluidima. Istraživani su zapreminski koeficijent prenosa mase u tečnoj fazi ( $k_L a$ ), koeficijent prenosa mase u tečnoj fazi ( $k_L$ ) i specifična međufazna površina ( $a$ ). pH je podešavana dodatkom hlorovodonične kiseline ili natrijum hidroksida. Utvrđeno je da se  $k_L a$  povećava sa povećanjem protoka gasa a smanjuje sa povećanjem prividne viskoznosti tečnosti. Za  $pH < 7$ , uticaj pH na prenos mase gas-tečnost je zanemarljiv. A kada je  $pH > 7$ , prenos mase se ubrzava sa povećanjem pH vrednosti. Istraživanje uticaja pH na  $k_L$  i a utvrđeno je da je promena prenosa mase pri  $pH > 7$  uzrokovana razgradnji molekulske strukture ksantana hidroksilnim jonima.*

*Ključne reči: barbotaza mehura, rastvor ksantana, nenjutnovski fluidi, pH, prenos mase.*